

# Reliability Analysis and Neural-network Modeling of Ship Radar Mast Structure by Adopting Quasi-random Sampling

Chang-Yong Song<sup>1</sup>

<sup>1</sup>Professor, School of Mechanical & Ocean Engineering, Mokpo National University, Jeonnam, Korea

**KEYWORDS:** Statistical reliability analysis, Neural-network modeling, Quasi-random sampling, Ship radar mast structure, Vibration and structure analysis

**ABSTRACT:** Outfitting structures, such as ship radar masts, require a design that considers the vibration and structural strength performance to ensure safe navigation. Nevertheless, reliability analysis considering design uncertainties is required because of the lack of classification rules for such structure design. This study examined the quasi-random sampling process suitable for the design reliability evaluation of radar masts. Neural network modeling was performed for the approximation using quasi-random sampling data regarding the vibration and structural strength performance of radar masts. For statistical reliability analysis, the Sobol sequence method was applied to the sampling process, and the reliability probability with the variation of the sampling number was evaluated. The approximate accuracy of neural network modeling was analyzed according to the variation of sampling number. In the context of research results, setting the quasi-random sampling number to approximately 0.4% of the Monte Carlo Simulation (MCS) sampling number allowed for a practical design reliability evaluation. A sampling number of approximately 0.2% of the MCS sampling number was found to be sufficient to approximate. Through this study, a quasi-random sampling process suitable for statistical reliability analysis of radar mast structures was determined, and a neural network model with high approximate accuracy was generated.

## 1. Introduction

A ship radar mast is an outfitting structure accommodating navigational communication equipment such as radar scanners and antennas. Excessive vibrational responses or structural damage to a radar mast can compromise navigation safety. Despite this, clear international classification society regulations or guidelines regarding the design of ship radar masts are not well established, leading to a reliance on empirical design practices. Therefore, statistical reliability analysis that considers design uncertainties is needed to determine the design safety of outfitting structures like the ship radar mast. Various studies have evaluated the design for the safety of ships and offshore structures using reliability analysis methods.

Eamon and Rais-Rohan (2009) performed a reliability-based design optimization (RBDO) considering parametric uncertainties to implement the probabilistic design of a composite submerged structure. Song and Choung (2011) proposed a probabilistic optimal design that minimizes the design risk by developing a constraint-feasible approximation model based on the moving least squares theory for the RBDO of riser apparatus design on floating production,

storage, and offloading units. Bai et al. (2015) performed a Monte Carlo simulation using finite element analysis and response surface method for the reliability analysis of lightweight submarine pipelines. Yin et al. (2018) proposed a non-probabilistic reliability model and sensitivity evaluation of the valve port plate of a seawater hydraulic pump for deep sea equipment. Cao et al. (2021) conducted the time-dependent reliability analysis of linear offshore structures using the pole-residue method, including the explicit closed-form solutions for nonstationary response variances under waves and earthquakes. Kamel et al. (2021) developed a reliability optimization method that incorporates the concept of reliability into the optimization process to determine the optimal configuration for a 2 MW offshore wind turbine model, considering the interaction between the soil and the structure. Shittu et al. (2022) conducted a stochastic sensitivity assessment of a typical offshore wind turbine jacket-type support structure, considering various limit states and stochastic variables and combining parametric finite element analysis (FEA) modeling, response surface modeling, and reliability analysis.

This study evaluated a quasi-random sampling process suitable for statistical reliability analysis considering the vibration and structural

Received 15 November 2024, revised 31 December 2024, accepted 6 January 2025

Corresponding author Chang-Yong Song: +82-61-450-2732, [cysong@mokpo.ac.kr](mailto:cysong@mokpo.ac.kr)

© 2025, The Korean Society of Ocean Engineers

This is an open access article distributed under the terms of the creative commons attribution non-commercial license (<http://creativecommons.org/licenses/by-nc/4.0>) which permits unrestricted non-commercial use, distribution, and reproduction in any medium, provided the original work is properly cited.

strength performance to ensure the structural design safety of a ship radar mast. The probability of reliability and the accuracy of a neural network model under quasi-random sampling conditions were compared. The probability of reliability was calculated by configuring the design thickness of the main structural members of the ship radar mast as the random variables adopting manufacturing tolerance standards and considering the vibration and structural strength performance as probabilistic performance functions. The vibration performance was defined as the natural frequency range of a ship radar mast that can avoid resonance with the major excitation forces from the main engine and propeller. The strength performance was estimated by setting the design load conditions according to the wind load and ship motion load specified in the International Classification Society regulations. The maximum combined stress was assessed based on the allowable yield stress criterion. The vibration and structural strength performance were evaluated using the finite element method (FEM). The Sobol sequence method was applied in the quasi-random sampling process, and the sampling frequency, the probability distribution of the probabilistic performance function, and the efficiency of numerical computations were examined based on an accuracy criterion of  $\pm 5\%$  with a 95% confidence level. The appropriate number of quasi-random sampling iterations for the statistical reliability analysis of the ship radar mast was determined by comparing it with the Monte Carlo simulation results. A neural network model was used to examine the relationship between the design space approximation characteristics and sampling conditions. The sampling conditions that can approximate the structural design space of a ship radar mast with the highest accuracy were determined using the neural network model. This paper is organized as follows. Section 2 briefly summarizes the theoretical background of the quasi-random sampling and neural network model applied in this study. Section 3 presents the results of the FEM-based vibration and structural strength performance evaluation, statistical reliability analysis, and neural network model-based approximation results. Finally, the main research findings are summarized in the conclusion.

## 2. Theoretical Background

### 2.1 Quasi-Random Sampling

The quasi-random sampling method is a statistical reliability analysis technique that can evaluate the uncertainty of a probabilistic performance function because of random variables at a low computational cost, provided that an appropriate number of samples consistent with the target reliability probability is applied. The Sobol sequence method is a quasi-random sampling method developed to enable uniform sampling with a small number of samples in the design space (Sobol and Levitan, 1999; Saltelli et al., 2010; Song, 2020). A Sobol sequence is generated by combining binary fractions of bit length  $w$  and direction numbers  $v_i^j$ , and the direction numbers are generated from the following primitive polynomial and recursive polynomial:

$$p_j(x) = x^q + a_1 x^{q-1} + \dots + a_{q-1} x + 1 \quad (1)$$

$$v_i^j = a_1 v_{i-1}^j \oplus a_2 v_{i-2}^j \oplus \dots \oplus a_{q-1} v_{i-q+1}^j \oplus v_{i-q}^j \oplus \frac{v_{i-q}^j}{2^q}, \quad i > q \quad (2)$$

where  $\oplus$  denotes the bitwise XOR operator. The Sobol sequence in the  $j^{\text{th}}$  dimension is defined as follows:

$$x_q^j \left( n = \sum_{i=0}^w b_i 2^i, \quad b_i \in \{0, 1\} \right) \quad (3)$$

Eq. (3) is organized as follows by applying the primitive polynomial in each dimension:

$$x_n^j = b_1 v_1^j \oplus b_2 v_2^j \oplus \dots \oplus b_w v_w^j \quad (4)$$

In the Sobol sequence method, the number of samples is determined using the following equation:

$$N_T = N_s(m+1), \quad \text{where } N_s = 2^k, \quad k = 1, 2, 3, \dots \quad (5)$$

where  $m$  is the number of random variables. The number of samples is determined by the complexity of the problem and the number of random variables. Therefore, it is necessary to review a reasonable number of samples according to the characteristics of the problem being evaluated for reliability using the Sobol sequence method.

### 2.2 Neural-Network Model

An approximate model was used to examine the design space because it can maximize computational efficiency when applied to design optimization or reliability analysis, which require high computational costs. In addition, the approximate model accuracy was determined by the generation conditions of the sampling data in the design space and the approximation method. This study used a neural network model as the approximation method to compare the accuracy of design space exploration under quasi-random sampling conditions. The neural network model was constructed using the elliptical basis function (EBF). The EBF neural network model (Luo et al., 2004) is a class of artificial neural networks that employ an elliptical basis function as an activation function. The structure of the EBF neural network model includes an input layer, a hidden layer with a non-linear activation function, and a linear output layer. An EBF neural network model with  $N$  hidden neurons can be expressed as follows:

$$f(x) = \sum_{i=1}^N w_i \phi(x, c_i, \Sigma_i) + b \quad (6)$$

where  $x$  is the input vector;  $w_i$  are the weights;  $b$  is the bias term;  $\phi(x, c_i, \Sigma_i)$  represents the elliptical basis function centered at  $c_i$  with a covariance matrix  $\Sigma_i$ . The elliptical basis function can be defined as follows:

$$\phi(x) = \exp\left(-\frac{1}{2}(x-c)^T \Sigma^{-1}(x-c)\right) \quad (7)$$

The EBF allows the neural network model to handle data with anisotropic properties and varying scales along different dimensions, enhancing flexibility and performance in complex pattern recognition and function approximation tasks.

### 3. Statistical Reliability Analysis and Approximation Results

#### 3.1 Vibration and Strength Performance

A ship radar mast is commonly installed on crude oil tankers with a dead weight tonnage (DWT) exceeding 100,000 and bulk carriers exceeding 180,000 DWT. Table 1 lists the main ship particulars.

**Table 1** Main ship particulars

| Category           | Contents                   | Particulars                    |
|--------------------|----------------------------|--------------------------------|
| Ship type          | Cargo type                 | Bulk carrier, Crude oil tanker |
|                    | DWT                        | 100,000–180,000                |
| Main dimension (m) | Length overall             | 250–290                        |
|                    | Breadth                    | 45                             |
|                    | Depth                      | 20–25                          |
| Main Engine        | Engine type                | two strokes                    |
|                    | No. of cylinder            | 6                              |
|                    | Power at MCR <sup>1)</sup> | 15,500 kW at 70 rpm            |
|                    | Power at NCR <sup>2)</sup> | 12,010 kW at 64 rpm            |
| Propeller          | Propeller type             | Fixed pitch propeller          |
|                    | No. of blades              | 4                              |

<sup>1)</sup>MCR: Maximum continuous rating

<sup>2)</sup>NCR: Normal continuous rating

Considering the high cost and significant time investment required for statistical reliability analysis and approximation processes, it is appropriate to evaluate the vibration and strength performance through numerical analysis using the FEM. Fig. 1 presents the design specifications and FEM model of the ship radar mast. The ship radar mast is represented by a three-dimensional FEM model, produced using shell elements and concentrated mass elements, comprising 129,428 nodes and 131,513 elements (Fig. 1). The material properties of ASTM A283-C steel, with a density of 7,850 kg/m<sup>3</sup>, elastic modulus of 210 GPa, Poisson's ratio of 0.3, and yield strength of 313 MPa, were applied to the FEM model to ensure that the weight of the FEM model matched the actual weight.

The boundary conditions applied in the vibration and strength analysis were implemented by constraining all degrees of freedom at the lowermost nodes of the radar mast of ships. The vibration analysis was conducted via a normal mode analysis with fixed boundary conditions and without additional loads to determine resonance with the major excitation frequencies. The strength analysis for the structural safety was performed by calculating the von Mises stress for each load case, derived from the wind load and ship motion acceleration as specified by the classification society regulations (KR, 2023), and comparing these stresses with the allowable yield stress. The wind load,  $F$ , was calculated using the following equation:

$$F = PA \times 10^{-3} (kN), \quad \text{where } P = \frac{1}{16} C_h C_s g V^2 (Pt) \quad (8)$$

where  $P$  is the wind pressure;  $A$  (m<sup>2</sup>) is the area sum of structural members under wind pressure in projection in respective wind direction;  $C_h$  is the height factor;  $C_s$  is the shape factor to be determined depending on the shapes of main parts;  $g$  (m/s<sup>2</sup>) is the

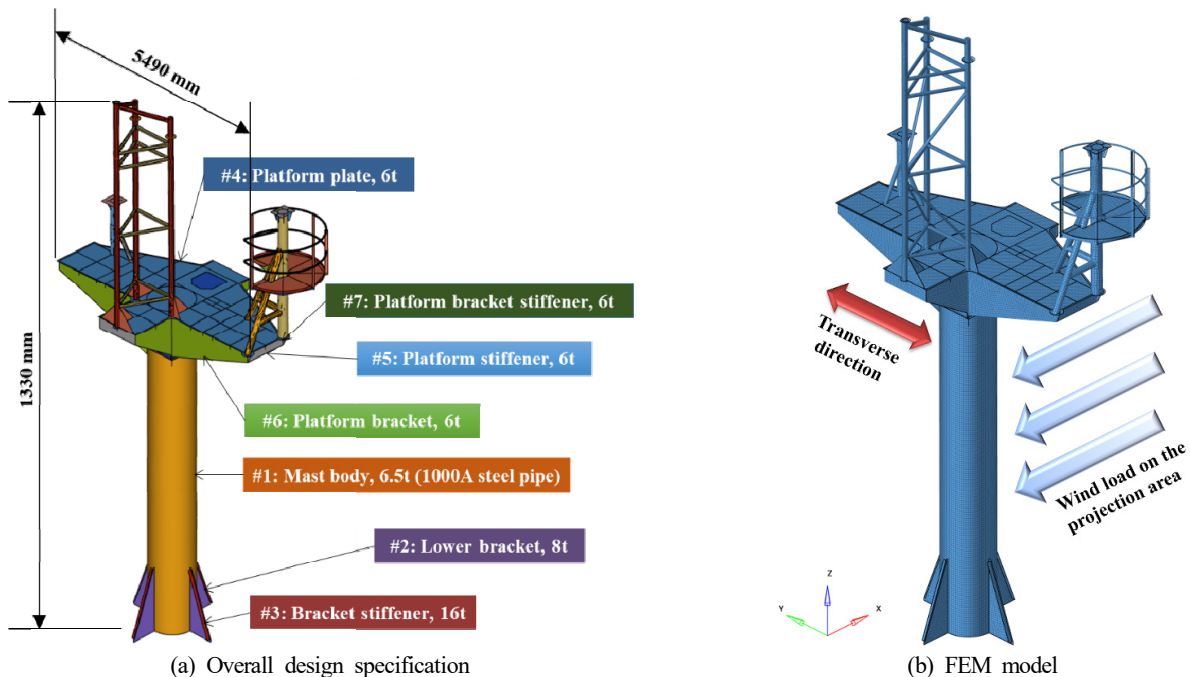


**Fig. 1** Design specifications and numerical model of the ship radar mast

**Table 2** Strength analysis results

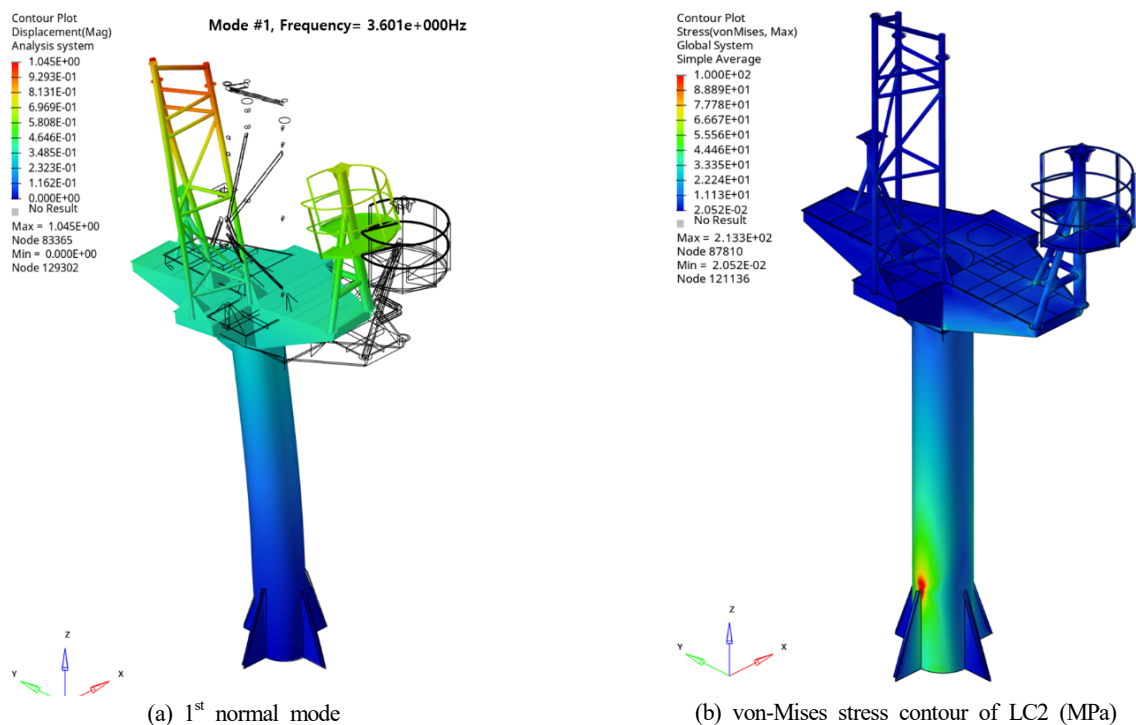
| # of load case | Wind load (kN) | Ship motion acceleration  | Max. von-Mises stress (MPa) | Max. stress location  |
|----------------|----------------|---|-----------------------------|---|
| LC1            | 585            | 1.0 <i>g</i> (N <sup>1)</sup> ) & 0.5 <i>g</i> (L <sup>2)</sup> ) | 73.1                        | Connection area between the lower part of the main body and the upper part of the lower bracket |
| LC2            |                | 1.0 <i>g</i> (N) & -0.5 <i>g</i> (L)                              | 213.3                       |   |
| LC3            |                | -1.0 <i>g</i> (N) & 0.5 <i>g</i> (L)                              | 65.5                        |   |
| LC4            |                | -1.0 <i>g</i> (N) & -0.5 <i>g</i> (L)                             | 202.3                       |   |
| LC5            |                | 1.0 <i>g</i> (N) & 0.5 <i>g</i> (T <sup>3)</sup> )                | 144.2                       |   |
| LC6            |                | 1.0 <i>g</i> (N) & -0.5 <i>g</i> (T)                              | 142.3                       |   |
| LC7            |                | -1.0 <i>g</i> (N) & 0.5 <i>g</i> (T)                              | 140.4                       |   |
| LC8            |                | -1.0 <i>g</i> (N) & -0.5 <i>g</i> (T)                             | 132.8                       |   |

<sup>1)</sup>N: Normal to the ship deck (SD). <sup>2)</sup>L: Longitudinal direction parallel to the SD. <sup>3)</sup>T: Transverse direction parallel to the SD.

acceleration due to gravity;  $V$  (m/s) is the design wind velocity. The wind load calculated with  $C_h = 1.3$ ,  $C_s = 0.7$ , and  $V = 51.5$  m/s for the ship radar mast using Eq. (8) was 585 kN, and the calculated wind load was applied to the FEA model in the form of pressure on the projection area against the sailing direction of the ship as shown in Fig. 1(b). The accelerations used to calculate the dynamic loads due to ship motion are the combination of  $\pm 1.0 g$  and  $\pm 0.5 g$  in the translational direction. Eight load cases were constructed considering the wind load and ship motion accelerations; Table 2 lists the maximum von Mises stress for each load case.

The vibration and strength analyses were performed using the general-purpose FEM program MSC.NASTRAN (Hexagon, 2023). Fig. 2 presents representative results, including the first normal mode shape and the stress contour of LC2, which exhibited the highest von Mises stress. The location of the maximum stress was the same in all load cases at the connection between the lower part of the main body

and the upper part of the lower bracket. The first normal mode was determined to be a transverse mode at 3.6 Hz (Fig. 2(a)). The potential for resonance between the first normal mode frequency of the ship radar mast and major excitation frequencies was assessed using a Campbell diagram (Campbell, 1924), as shown in Fig. 3. The 3.6 Hz normal mode frequency does not resonate within the NCR to MCR range, where most voyages occur (Fig. 3). Considering various uncertainties, the resonance is predicted to be avoided within the NCR to MCR range if the design target for the first normal mode frequency of the ship radar mast is set in the range of 3.6 to 4.0 Hz. Higher upper-frequency limits can improve the stiffness, but if the upper-frequency limit is higher than 4.0 Hz, resonance with the propeller first or main engine fourth excitation frequency may occur near the NCR. The maximum stress of LC2, calculated at 213.3 MPa, occurred at the connection between the lower part of the main body and the upper part of the lower bracket, as shown in Fig. 2(b). The

**Fig. 2** Normal mode and strength analysis results

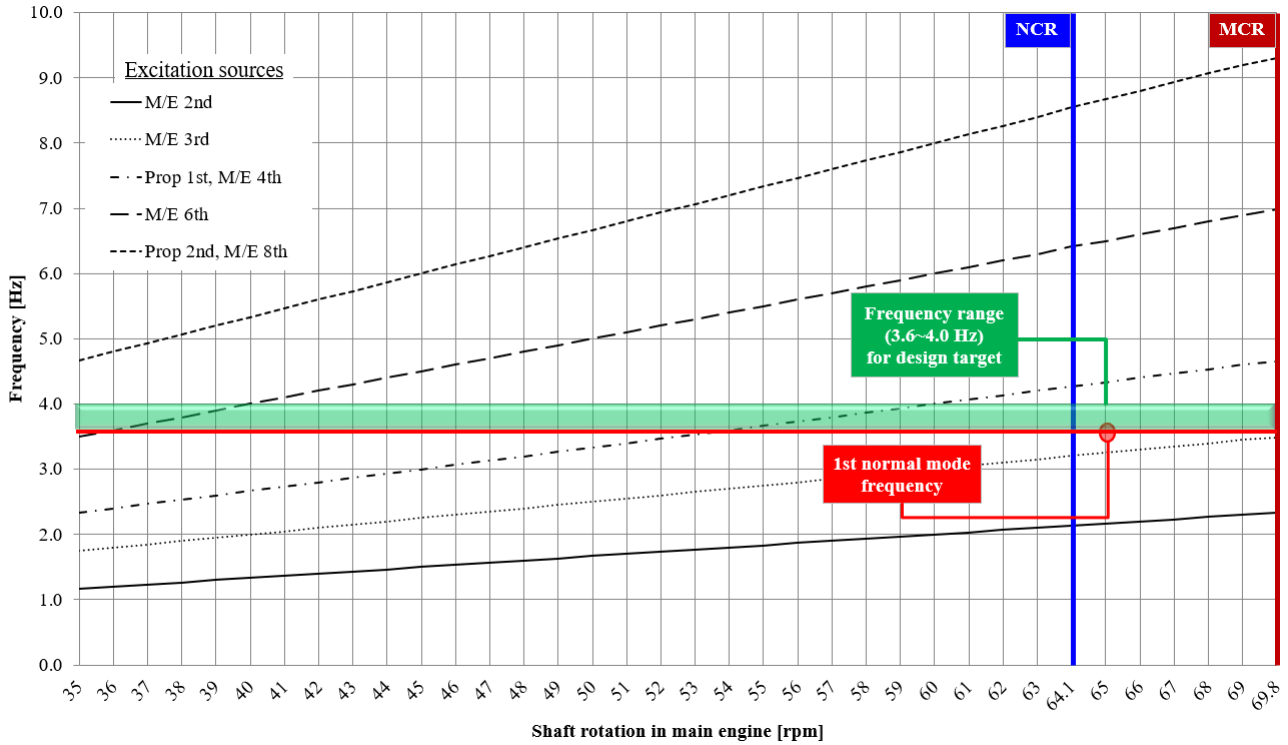


Fig. 3 Campbell diagram diagnosis results

allowable stress was set to 85% of the material yield stress, according to the regulations of the classification society, resulting in an allowable stress of 266.05 MPa. Although the maximum stress was below the allowable stress of 266.05 MPa, the safety margin was only 19.8%, suggesting that the strength performance was not sufficiently high. Based on the vibration and strength performance evaluation, the current ship radar mast requires a detailed review of the design reliability through an appropriate statistical reliability analysis.

### 3.2 Statistical Reliability Analysis

The Sobol sequence method was applied in the statistical reliability analysis to identify a suitable quasi-random sampling process for evaluating the design reliability related to the vibration and strength performance of the ship radar mast. The limit state for the probabilistic performance function concerning vibration performance was set in the range of 3.6 to 4.0 Hz, and it was set at the allowable yield stress of 266.05 MPa for strength performance. The reliability of the defined

probabilistic performance functions was assessed based on a 1.0% failure probability. The probability of reliability was estimated with an accuracy of  $\pm 5\%$  at a 95% confidence level, which is the reliability of the lower and upper bounds. The design uncertainty of the ship radar mast was considered as the manufacturing tolerance of the seven major component thicknesses shown in Fig. 1(a) and was adopted as a random variable. The standard deviation of the random variable was set by referring to the manufacturing tolerance standards (ASTM, 2008; KS, 2019), and the probability distribution function was defined to follow a normal distribution (Navidi, 2008; NIST/SEMATECH, 2003), as listed in Table 3.

In the quasi-random sampling process, the number of samples was set in five cases by sequentially varying the integer  $k$  in Eq. (5) from 5 to 9 considering the  $\pm 2$  range for the number of random variables, resulting in 192 times (Case-I), 384 times (Case-II), 768 times (Case-III), 1,536 times (Case-IV), and 3,072 times (Case-V). The probability of reliability for each case was compared with the results of

Table 3 Definition of random variables

| Random variable | Standard deviation | Distribution type | Design variable | Lower bound (mm) | Initial design (mm) | Upper bound (mm) |
|-----------------|--------------------|-------------------|-----------------|------------------|---------------------|------------------|
| $X_1$           | $\pm 12.5\%$       | Normal            | $x_1$ (#1)      | 3.5              | 6.5                 | 9.5              |
| $X_2$           | $\pm 6.1\%$        | Normal            | $x_2$ (#2)      | 6.0              | 8.0                 | 10.0             |
| $X_3$           | $\pm 6.9\%$        | Normal            | $x_3$ (#3)      | 12.0             | 16.0                | 20.0             |
| $X_4$           | $\pm 12.5\%$       | Normal            | $x_4$ (#4)      | 4.0              | 6.0                 | 8.0              |
| $X_5$           | $\pm 12.5\%$       | Normal            | $x_5$ (#5)      | 4.0              | 6.0                 | 8.0              |
| $X_6$           | $\pm 12.5\%$       | Normal            | $x_6$ (#6)      | 4.0              | 6.0                 | 8.0              |
| $X_7$           | $\pm 12.5\%$       | Normal            | $x_7$ (#7)      | 4.0              | 6.0                 | 8.0              |

the Monte Carlo Simulations (MCSs) (Siddall, 1983), which require relatively large-scale sampling but offer high accuracy in reliability evaluation. The required number of MCS samples ( $N_{p_f}$ ) for estimating the probability of reliability was calculated using the following equation:

$$N_{p_f} = 200^2 \left[ \frac{(1-p_f)}{e} \right] \quad (9)$$

where  $p_f$  is the target probability of failure and  $e$  is the error ratio of accuracy based on the 95% confidence level. From Eq. (9), the number

of MCS samples was set to 792,000. Table 4 lists the results of the statistical reliability analysis for the vibration and strength performance of the ship radar mast based on the application of quasi-random sampling and MCS considering the 0.00001 convergence tolerance.

The quasi-random sampling conditions of Case-V yielded the same probability of reliability results as the MCS, as listed in Table 4. For cases with fewer samples than Case-III, however, the error compared to the MCS increased, and the probability of reliability tended to be overestimated. The probability of reliability for the lower limit of vibration was lower than that of the other probabilistic performance

**Table 4** Statistical reliability analysis results

| Item     | Probability of reliability (%)  |   |  |
|----------|---|---|--|
|          | Lower limit of vibration<br>(1 <sup>st</sup> normal mode frequency $\geq$ 3.6 Hz) | Upper limit of vibration<br>(1 <sup>st</sup> normal mode frequency $\leq$ 4.0 Hz) | Strength<br>(Max. stress $\leq$ 235 MPa) |
| Case-I   | 91.4  | 99.5  | 98.4                                     |
| Case-II  | 91.4  | 99.5  | 98.4                                     |
| Case-III | 90.8  | 99.6  | 98.4                                     |
| Case-IV  | 90.7  | 99.6  | 98.4                                     |
| Case-V   | 90.5  | 99.5  | 98.3                                     |
| MCS      | 90.5  | 99.5  | 98.3                                     |

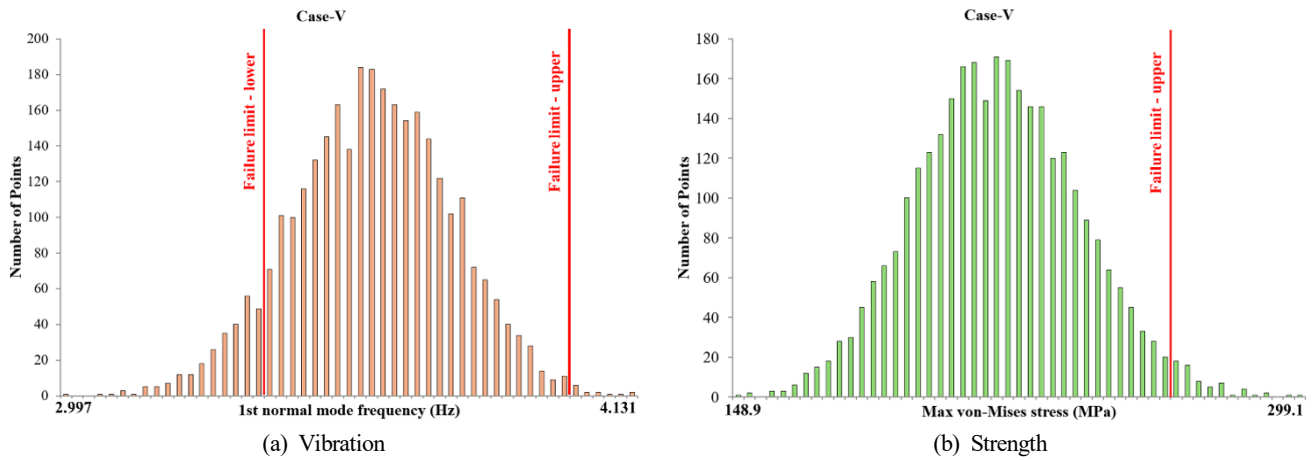


**Fig. 4** SFH results for Case-V

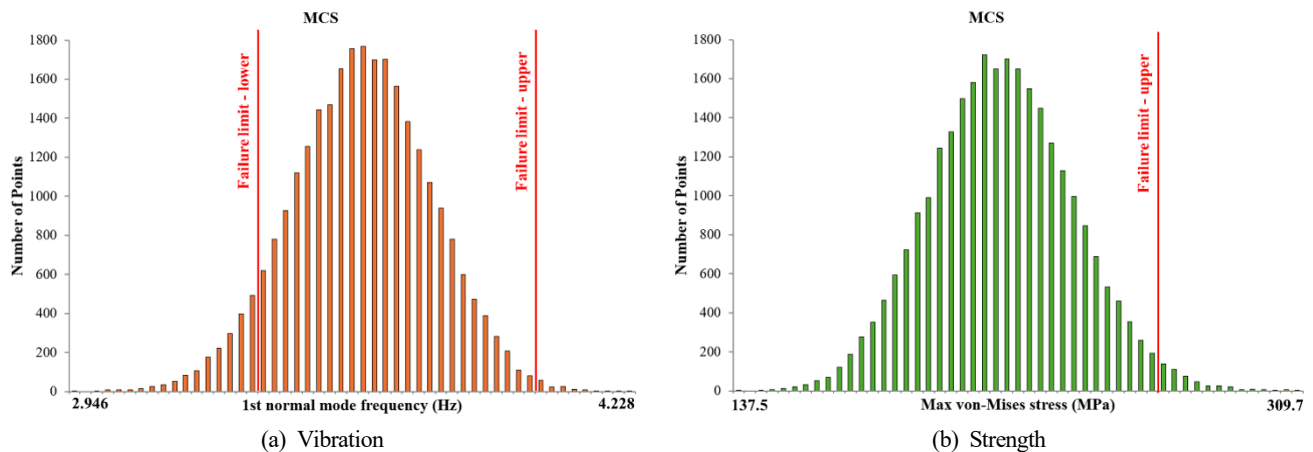


**Fig. 5** SFH results for MCS

functions. This result can be attributed to the initial value of the first normal mode frequency being actively close to the lower limit of vibration. The effective probability of reliability for the lower limit of vibration, the upper limit of vibration, and the strength of the ship radar mast were estimated to be 90.5%, 99.5%, and 98.3%, respectively. Figs. 4 and 5 present the statistical frequency histogram (SFH) results for each probabilistic performance function for Case-V and MCS.

The distribution characteristics of the SFH for Case-V and MCS were almost identical (Figs. 4 and 5). In the SFH, the height of the histogram was proportional to the frequency of occurrence of the characteristic values of the corresponding probabilistic performance function. A quasi-random sampling number of approximately 0.4% of the MCS sampling number was sufficient for the statistical reliability analysis of the ship radar mast, as shown in Table 4 and Figs. 4 and 5. Hence, applying the Sobol sequence method-based quasi-random sampling to the statistical reliability analysis of the ship radar mast can achieve high numerical computational efficiency.

### 3.3 Approximation

This section reports the correlation between the sampling conditions applied in the statistical reliability analysis and the accuracy of the EBF neural network model. Fig. 6 presents the structure of the EBF neural network model used in this study, including the input, hidden, and output layers.

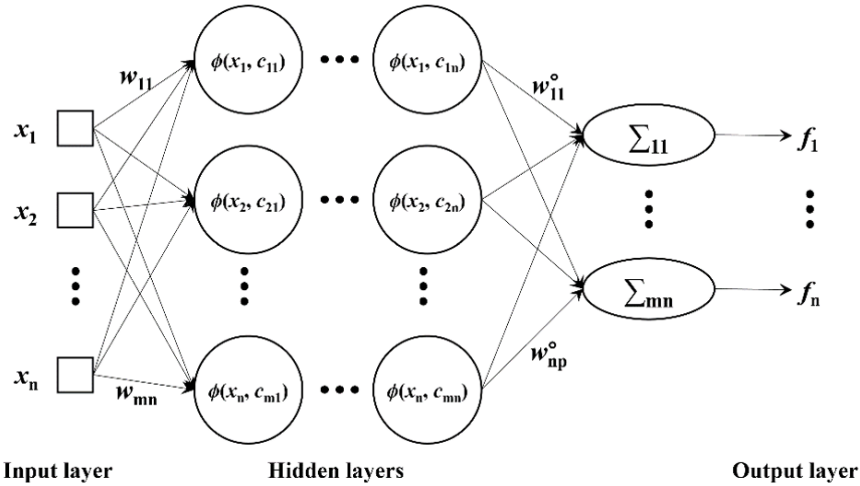


Fig. 6 Structure of the EBF neural network model

Table 5 Approximation results based on EBF neural network model

| Item     | $R^2$ value for vibration<br>(1 <sup>st</sup> normal mode frequency) | $R^2$ value for strength<br>(Max. von-Mises stress) | Averaged $R^2$ value |
|----------|--|---|----------------------|
| Case-I   | 0.923  | 0.958   | 0.940                |
| Case-II  | 0.923  | 0.959   | 0.941                |
| Case-III | 0.961  | 0.930   | 0.946                |
| Case-IV  | 1.000  | 1.000   | 1.000                |
| Case-V   | 1.000  | 1.000   | 1.000                |
| MCS      | 1.000  | 1.000   | 1.000                |

The seven design variables were placed in the input layer (Fig. 6); three hidden layers were used, and the probabilistic performance functions of vibration and strength were applied to the output layer. The convergence was set as a learning rate of 0.7 and ten training iterations. In addition, the model aims to identify the most suitable conditions for approximating the vibration and strength performance of the radar mast of ships. The approximation accuracy of the EBF neural network model was determined using the  $R^2$  value, which is expressed as follows:

$$R^2 = 1 - \frac{\sum (t_i - y_i)^2}{\sum (t_i - \bar{t}_i)^2} \quad (10)$$

where  $t_i$  represents the actual values;  $y_i$  represents the predicted values from the EBF neural network model;  $\bar{t}_i$  represents the mean of the actual values. An  $R^2$  value of 1.0 suggests that the predictions from the EBF neural network model perfectly match the actual values across the entire design space. Table 5 lists the approximation fidelity of the EBF neural network model.

Case-IV, Case-V, and MCS exhibited  $R^2$  values closest to 1.0, indicating the highest approximation accuracy across the design space (Table 5). The approximation results for Case-I and Case-II showed negligible differences, with an error rate of approximately 6% compared to the averaged  $R^2$  results of MCS, while Case-III exhibited an error rate of 5.4%. Although the differences in approximation

accuracy were observed across the sampling conditions, all cases showed sufficient accuracy for use as approximate models to estimate the design space. Thus, the increase in sampling frequency applied in statistical reliability analysis showed a significant correlation with the accuracy of the EBF neural network model. Based on the results in Table 5, an effective sampling frequency for the EBF neural network model-based approximation of the ship radar mast, using quasi-random sampling, was approximately 0.2% of the MCS sampling frequency.

#### 4. Conclusions

The Sobol sequence method was applied to develop a suitable quasi-random sampling process for the statistical reliability analysis of the vibration and structural strength performance of a ship radar mast. The probability of reliability was evaluated under varying sampling conditions. In addition, the correlation between the changes in sampling conditions applied in the statistical reliability analysis and the approximation accuracy of the EBF neural network model was investigated. The probability of reliability was calculated by configuring the design thickness of the main structural components of the ship radar mast as random variables, adopting manufacturing tolerance standards. The vibration and strength performances were applied as probabilistic performance functions. The design target for vibration performance was defined as a first normal mode frequency in the 3.6 to 4.0 Hz range to avoid resonance with major excitation forces from the main engine and propeller across the NCR to MCR range. For strength performance, eight design load conditions were selected based on wind load and ship motion load specified by International Classification Society regulations. The maximum von Mises stress was calculated, and the estimated safety margin under the most severe design load condition was 19.8% based on the allowable yield stress.

The Sobol sequence method was used to explore a quasi-random sampling process suitable for evaluating the design reliability of vibration and strength performance. The probability of reliability for vibration and strength performance was estimated with an accuracy of  $\pm 5\%$  at a 95% confidence level. Setting the quasi-random sampling number to approximately 0.4% of the MCS sampling number allowed for a practical design reliability evaluation with high computational efficiency. The effective probabilities of reliability for the lower limit of vibration, upper limit of vibration, and strength of the ship radar mast were estimated to be 90.5%, 99.5%, and 98.3%, respectively. The correlation between the sampling conditions applied in the statistical reliability analysis and the accuracy of the EBF neural network model was also examined. An increase in the quasi-random sampling number revealed a significant correlation with the accuracy of the EBF neural network model. A sampling number of approximately 0.2% of the MCS sampling number was sufficient to approximate the structural design space of the ship radar mast with high accuracy.

These results suggest that statistical reliability analysis and the EBF neural network model, when applying a reasonable quasi-random

sampling process, can be utilized effectively for design reliability evaluations and design space approximations of similar ship and offshore structure-outfitting components.

#### Conflict of Interest

Chang-Yong Song serves as a journal publication committee member for the Journal of Ocean Engineering and Technology, but he did not have a role in the decision to publish this article. There are no potential conflicts of interest relevant to this article.

#### Funding

This Research was supported by Research Funds of Mokpo National University in 2022.

#### References

- ASTM. (2008). *Standard specification for seamless, welded, and heavily cold worked steel pipes*.
- Bai, Y., Tang, J., Xu, W., & Ruan, W. (2015). Reliability-based design of subsea light weight pipeline against lateral stability. *Marine Structures*, 43, 107–124. <https://doi.org/10.1016/j.marstruc.2015.06.002>
- Campbell, W. (1924). Protection of steam turbine disk wheels from axial vibration. *Journal of Fluids Engineering*, 46, 31–140. <https://doi.org/10.1115/1.4058289>
- Cao, Q., Li, H., Li, H., & Liu, F. (2021). Time-dependent reliability analysis of fixed offshore structures under stochastic loadings. *Applied Ocean Research*, 117, 102901. <https://doi.org/10.1016/j.apor.2021.102901>
- Luo, J. C., Leung, Y., & Zheng, J. (2004). An elliptical basis function network for classification of remote sensing images. *Journal of Geographical Systems*, 6(1), 219–236. <https://doi.org/10.1007/s10109-004-0136-1>
- Eamon, C. D., & Rais-Rohani, M. (2009). Integrated reliability and sizing optimization of a large composite structure. *Marine Structures*, 22(2), 315–334. <https://doi.org/10.1016/j.marstruc.2008.03.001>
- Hexagon. (2023). *MSC.Nastran user manual*. Hexagon AB.
- Kamel, A., Dammak, K., Yangui, M., El Hami, A., Ben Jdidia, M., Hammami, L., & Haddar, M. (2021). Reliability optimization of a coupled soil structure interaction applied to an offshore wind turbine. *Applied Ocean Research*, 113, 102641. <https://doi.org/10.1016/j.apor.2021.102641>
- Korean Industrial Standards (KS). (2019). *Dimensions, weight and permissible variations of hot rolled steel plates, sheets and strip*. <https://www.kssn.net/search/stdetail.do?itemNo=K001010123803>
- Korean Register of Shipping (KR). (2023). *Rules and guidance for the classification of steel ships*.



- Navidi, W. (2008). *Statistics for Engineers and Scientists*. McGraw-Hill Higher Education.
- NIST/SEMATECH (2003). *Engineering Statistics Handbook*. National Institute of Standards and Technology. <https://doi.org/10.18434/M32189>
- Saltelli, A., Annoni, P., Azzini, I., Campolongo, F., Ratto, M., & Tarantola, S. (2010). Variance based sensitivity analysis of model output. *Computer Physics Communications*, *181*(2), 259–270.
- Shittu, A. A., Mehmanparast, A., Amirafshari, P., Hart, P., & Kolios, A. (2022). Sensitivity analysis of design parameters for reliability assessment of offshore wind turbine jacket support structures. *International Journal of Naval Architecture and Ocean Engineering*, *14*, 100441. <https://doi.org/10.1016/j.ijnaoe.2022.100441>
- Siddall, J. N. (1983). *Probabilistic engineering design*. Marcel Dekker Inc., New York.
- Sobol, I. M., & Levitan, Y. L. (1999). A pseudorandom number generator for personal computers. *Computers & Mathematics with Applications*, *37*(4–5), 33–40.
- Song, C. Y. (2020). Reliability analysis for structure design of automatic ocean salt collector using sampling method of Monte Carlo simulation. *Journal of Ocean Engineering and Technology*, *34*(5), 316–324. <https://doi.org/10.26748/KSOE.2020.054>
- Song, C. Y., Lee, J., & Choung, J. (2011). Reliability-based design optimization of an FPSO riser support using moving least squares response surface meta-models. *Ocean Engineering*, *38*(2–3), 304–318. <https://doi.org/10.1016/j.oceaneng.2010.11.001>
- Yin, F., Nie, S., Ji, H., & Huang, Y. (2018). Non-probabilistic reliability analysis and design optimization for valve-port plate pair of seawater hydraulic pump for underwater apparatus. *Ocean Engineering*, *163*, 337–347. <https://doi.org/10.1016/j.oceaneng.2018.06.007>

### Author ORCID

| Author name      | ORCID               |
|------------------|---------------------|
| Song, Chang-Yong | 0000-0002-1098-4205 |